Review of Computer Engineering Research
2022 Vol. 9, No. 4, pp. 209-221.
ISSN(e): 2410-9142
ISSN(p): 2412-4281
DOI: 10.18488/76.v9i4.3160

ADAPTIVE BEAMFORMING MODEL FOR 5G HIGH SPEED NETWORKS USING MILLIMETER WAVE COMMUNICATION IN UPLINK

Indrabhan Borse[1+]
Hitendra Patil[2]

[1,2]*Department of Computer Engineering, SSVPS B.S.Deore College of Engineering, KBC North Maharashtra University, Jalgaon, Maharashtra, India.*
[1]*Email: indrabhan2000@gmail.com*
[2]*Email: hitendradpatil@gmail.com*

(+ Corresponding author)

Article History
Received: 25 July 2022
Revised: 5 September 2022
Accepted: 27 September 2022
Published: 7 October 2022

Keywords
Adaptive beamforming
Millimeter wave communication
Salp-Bird Swarm Optimization
Shark Smell Optimization
Spectral efficiency systems.

ABSTRACT

Future generation cellular communications will require increased data rates and transmission using millimeter waves (MMWs), which are an emerging concept to meet this need. The MMW frequencies offer the potential for orders of magnitude capacity improvements. However, MMW network connections are more susceptible to blocking, and they suffer from rapid quality differential. The major limitation of offering multiconnectivity in MMWs is the necessity of tracking the direction of every link with its suitable timing and power. Beamforming enables wireless communications, even with higher frequency bands such as the MMW frequency band. The main purpose of this article is to develop an adaptive beamforming approach for 5G millimeter-wave networks. MMW communication efficiency is improved by enhancing the narrowband weights of adaptive beamforming. Here, the Shark Smell Optimization (SSO) and Bird Swarm Algorithm (BSA) are combined to improve the weight update approach of the new Salp-Bird Swarm Optimization (S-BSO) to achieve adaptiveness in beamforming. To demonstrate the effectiveness of the suggested Salp-Bird Swarm Optimization (S-BSO), an experimental comparison is carried out with the current models.

Contribution/Originality: A novel Salp-Bird Swarm Optimization (S-BSO) algorithm has been developed in this study to improve the bit error rate to enhance the efficiency of the adaptive beamforming algorithm.

1. INTRODUCTION

The key approaches for reaching a high 10 Gbit/s data rate are widely used in millimeter wave (MMW) communication. The MMW communication field has seen an increase in research activity in recent years [1]. In these studies, numerous MMW bands are utilized [2]. MMW bands, which typically range from 30 to 300 GHz and have a large amount of spectrum available to them, are the most significant and have drawn the attention of researchers because they offer the possibility of high Gbps data transfer rates to support seamless connectivity and low expectancy wireless facilities [3]. MMW communications might be different from standard microwave bands due to propagation properties [4]. Ecological factors, including rain, water vapor, and oxygen molecules, have a negative impact on MMW signal propagations and cause severe signal loss [5].

The penetration losses brought on by obstructions such as tress and structures can be more severe for low frequency signals and can even affect the MMW frequency compared to low frequency signals [6]. These obstructions may cause radically different route loss for propagation [7]. For the system analysis to guarantee the MMW networks' correctness and performance, certain elements and special characteristics are necessary [8]. Baseband is where all signal processing is done by one radio frequency (RF) circuit per antenna and is very complex and power-consuming to implement. In the study by Giordani, et al. [9], low-resolution analog-to-digital converters (ADCs) and hybrid beamforming (HBF) are two methods that address these issues and require less RF circuitry [10]. In contrast to full digital beamforming, hybrid beamforming separates the "baseband digital precoding and the analogue beamforming" created at the RF field into two distinct parts [11]. Therefore, beamforming has to be aware of the specifics of the arbitrary wireless channel. The sparsity of the MMW channel has recently been used to solve the issue of channel estimation in MMW systems using a variety of methods [12]. A beamforming codebook design for a phased array antenna was used to create a hybrid structure Alkhateeb, et al. [13].

An orthogonal matching pursuit (OMP) approach was also used to obtain a specific estimate of the reference beamforming vector in good agreement with the hybrid structure [14].

A hybrid construction with a phased array antenna requires a greater number of RF chains in order to realize reliable estimations of the reference beamforming vector.

For a single chain RF antenna, the subarray beamforming scheme is performed [15]. To ensure that the proposed exposure zone and the real region of the 3D beamforming have no discernible differences, a sub-array-based beamforming framework has been devised [16].

2. SYSTEM MODEL AND BEAMFORMING IN MILLIMETER WAVE COMMUNICATION SYSTEM

Figure 1 contains a diagrammatic depiction of a point-to-point narrowband MMW communication system where data streams M_d are forwarded and gathered through receiver antennas M_{rs} and transmit antennas M_t , respectively. Here, both receiver and transmitter are equipped with RF chains M_{RF} , in which $(M_{rs}, M_t) >> M_{RF}$. A symbol vector $M_d \times 1$ is indicated by d through $Er\{dd^H\} = Ir_{M_d}$ precoded into $M_{RF} \times M_d$, a digital beamforming matrix $M_{RF} \times M_d$, and then precoded into an analog beamforming matrix developed through phase shifters in the analog circuitry. Based on the baseband representation, the transmit antenna array computes the precoded signal vector. Given as $v = S_{RF} S_{BC} d$, the fixed normalized transmit power restriction is $tr\left(S_{RF} S_{BC} S_{BC}^H S_{RF}^H\right) \leq 1$ without loss of generality.

In Treichler and Agee [17], a geometry-based channel model is used to characterize the MMW propagation channel with rays M_{RS} and clusters M_{CS} . Equation 1 presents the channel matrix H , which is computed by using the MMW system with the transmitter and the receiver through a half-wave spaced uniform linear array.

$$H = \sqrt{\frac{M_t M_{rs}}{M_{CS} M_{RS}}} \sum_{i=1}^{M_{CS}} \sum_{j=1}^{M_{RS}} \beta_{ij} \zeta_{rs}\left(\theta_{ij}^{rs}\right) \zeta_t\left(\theta_{ij}^{t}\right)^H \tag{1}$$

Equations 2 and 3 argue the angles of departure and arrival, represented as θ_{ij}^t and θ_{ij}^{rs} , respectively. The responses of the transmitter and receiver antenna arrays to the i^{th} cluster in the j^{th} ray are described and the complex gains of the i^{th} cluster in the j^{th} ray are referred to as β_{ij} .

$$\zeta_{rs}\left(\theta_{ij}^{rs}\right) = \frac{1}{\sqrt{M_{rs}}} \left[1 e^{j\pi \sin \theta_{ij}^{rs}} \cdots e^{j\pi (M_{rs}-1) \sin \theta_{ij}^{rs}}\right]^T \tag{2}$$

$$\zeta_t\left(\theta_{ij}^{t}\right) = \frac{1}{\sqrt{M_t}} \left[1 e^{j\pi \sin \theta_{ij}^{t}} \cdots e^{j\pi (M_t-1) \sin \theta_{ij}^{t}}\right]^T \tag{3}$$

In the final stage, the processed signal is calculated taking hybrid analog and digital beamforming into account at the receiver $M_{RF} \times M_{rs}$, an analog combiner Q_{RF} , with the $M_{RF} \times M_d$ digital base band combiner Q_{BC} as formulated in Equation 4.

$$x = Q_{BC}^H Q_{RF}^H H S_{RF} S_{BC} d + Q_{BC}^H Q_{RF}^H nv \qquad (4)$$

In Equation 4, the additive noise vector is given as nv at receive antennas M_{rs}, where $nv \sim O(0, \sigma^2 Ir_{M_{rs}})$, and the covariance matrix is termed as $\sigma^2 Ir_{M_{rs}}$.

Assume you have a uniform linear array with sensor components spaced about half the wavelength of the received signal. This representation describes the angle of the received signal as determined by the antenna's line of sight. Equation 5 presents the output signal of the narrowband adaptive beamformer.

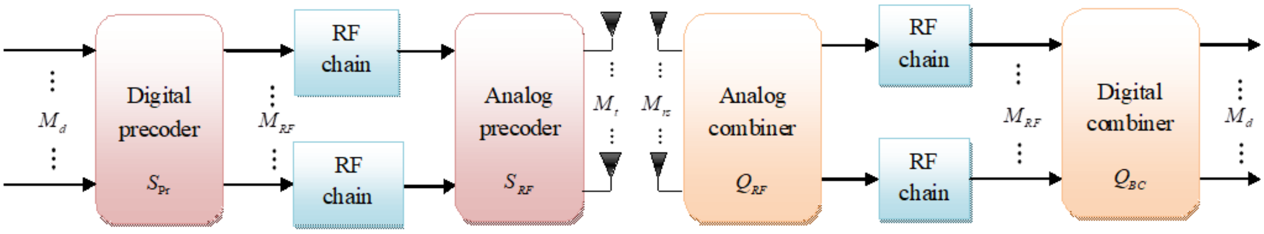

Figure 1. Structure of narrowband MMW communication.

$$x_k = w^H Y_k \qquad (5)$$

The time index is referred to as $w = [w_1, \cdots, w_M]^T \in CV^M$, the array observation vector is represented as $Y_k = [y_1, \cdots, y_M]^T \in CV^M$, $(\bullet)^H$ and $(\bullet)^T$ are used to represent the transposition and the Hermitian transpose, respectively. Additionally, Equation 6 formulates the complex vector of array observation Y_k.

$$Y_k = y_{sd} + y_i + ns \qquad (6)$$

Interference, intended signal, and array noise are referred to as y_i, y_{sd}, and ns in Equation 6. Equation 7 is used to provide the desired signal for narrowband.

$$y_{sd} = SD_k \alpha \qquad (7)$$

Terms SD_k and α denote the desired signal and the intended signal waveform, respectively.

3. LITERATURE SURVEY

Table 1 describes the methodology that has been adopted by various authors and the techniques they have followed in the implementation of their work, and some challenges are also identified.

Table 1. Review of conventional millimeter-wave cellular network models.

Author [citation]	Methodology	Features	Challenges
Liu and Bentley [18]	Beam tracking	• It improves the performance of a cellular network. • It develops an energy efficient network.	• This model is not applicable for designing control applications.
Muhammad, et al. [19]	FPC (fractional power control)	• It enhances performance. • The probability of the SINR (signal-to-interference-and-noise-ratio) coverage is improved.	• This model is restricted due to the use of open and closed loops.

Author [citation]	Methodology	Features	Challenges
Cheng, et al. [20]	Directional beamforming model	• It enhances the coverage performance in terms of smaller arrays. • It attains better accuracy.	• It achieves beam alignment errors that may degrade performance.
Asim, et al. [21]	Two-stage estimation algorithm	• It increases the performance. • It improves accuracy of estimation.	• It is affected due to the hardware complexity.
Sultan, et al. [22]	Fast 3D beamforming	• It reduces the search time of the beam. • It attains higher performance.	• It needs a considerably lower number of beam scans.
Satyanarayana, et al. [23]	Hybrid precoding	• It is computationally efficient. • It enhances the performance of this model.	• A major challenge in this model is its configuration in wideband systems.
Wang, et al. [24]	Optimal algorithm for hybrid beamforming	• It improves the performance of a cellular network. • It obtains optimal solution.	• It is affected due to propagation loss.
Kulkarni, et al. [25]	Precoding-combining algorithm	• It is proposed for improving the efficiency of this model.	• This model is compromised by insufficient channel state knowledge.

4. EXISTING 5G MILLIMETER WAVE COMMUNICATION SYSTEM

A. Constant Modulus Algorithm (CMA) Adaptive Beamformer

CMA is utilized for radio signal blind separation and equalization but its drawbacks is a poor convergence rate. Weights are updated in Treichler and Agee [17], as given in Equation 8.

$$w_{k+1} = w_k - 2\mu \cdot \varepsilon \cdot Y_k \tag{8}$$

μ represents the step size, and ε is the error signal or mean square error (MSE), which is stated as:

$$\varepsilon = MSE = \left(x_k - \frac{x_k}{|x_k|} \right) \tag{9}$$

The array output of the CMS is MSE because it distinguishes between the desired signal and the input signal.

$$x_{k(CMA)} = Y_k^T w_k = w_k^H Y_k \tag{10}$$

The weakness in the CMA is fixed by LS-CMS to accelerate the convergence time.

B. LS-CMS (Least Squares Constant Modulus Algorithm) Adaptive Beamformer

The weight update equation is formulated in Agee [26] based on the offset vector, as per Equation 11:

$$\Im = -\left[\hat{G}_w G_w^H\right]^{-1} \hat{G}_w \phi \tag{11}$$

The data sample of one block is indicated by K, the complex Jacobian ϕ is shown as $\hat{G}_w$, and the data sample error is shown as $\phi = [\phi_1, \cdots, \phi_K]^T$, as stated in Equation 12.

$$\hat{G}_w = \left[\nabla \hat{G}_1, \cdots, \hat{G}_K\right] \tag{12}$$

Finally, the LS-CMS weight update is displayed as:

$$\begin{aligned} w_{k+1} &= w_k - \Im \\ &= w_k - \left\{\left[\hat{G}_w G_w^H\right]^{-1} \hat{G}_w \phi\right\} \end{aligned} \tag{13}$$

The aim of this upgrade is to increase the convergence rate.

5. PROPOSED ADAPTIVE BEAMFORMING TECHNIQUE

In order to outperform the currently available beamforming algorithms, a novel S-BSO algorithm is developed. The convergence rate is the main issue in the adaptive beamforming strategy in millimeter-wave communication systems. By decreasing the bit error rate in millimeter-wave communication systems, improvement in convergence rate is observed. The proposed S-BSO method is used in Equation 5 to optimize the weight w, whose bounding limit is between -50% and 50%. The previous weight w_k by the recommended S-BSO technique is expressed, and a fresh weight w_{k+1} is updated, as stated in Equation 14, by taking into consideration the response solution, indicated by the change in percentage, where the solution's length falls within the range of $1\times$ length of the primary weight.

$$w_{k+1} = w_k + \left(w_k \times \frac{sol}{100} \right) \tag{14}$$

A. Novel Salp-Bird Swarm Optimization

In order to improve the performance of millimeter wave communication, an innovative S-BSO approach is suggested for maximizing the weight of adaptive beamforming. The gains from BSA [27] and SSO [28] served as inspiration for this new method. The created approach takes into account the following scenario: if $E_3 < 0.5$ SSO is used to update the solution, otherwise BSA updating is used.

Algorithm start-up: When the shark detects the odor, the search procedure is started. The shark initially notices the milder odor, which is depicted as:

$$\left[w_1^1, w_2^1, w_3^1, \cdots, w_{NP}^1 \right] \tag{15}$$

Each solution marks an odor particle that represents a possible location of the shark in the early stages of the search. Here, NP represents the population's size, w_j^1 is the j^{th} starting location vector, where $j = 1,2,\ldots,NP$, and the solution is initially given by Equation 16.

$$w_j^1 = \left[w_{j,1}^1, w_{j,2}^1, .., w_{j,Dv}^1 \right] \tag{16}$$

In the abovementioned equation, the j^{th} shark location at the i^{th} measurement is termed by $w_{j,1}^1$, and the i^{th} decision variable of the j^{th} individual is given by w_j^1, in which $i = 1,2,..., Dv$, and Dv reveals how many choice variables there are in the optimization issues. Through an objective function in the SSO that takes into account the strength of the odor at each point, the proximity to the prey is calculated. When the objective function, which determines the most ideal candidate solution for prey, has a greater value, a stronger odor is detected.

Shark's movement toward its prey: Because velocity is important for getting there, it is calculated at every location. Equation 17 computes the initial velocity vector using the location vectors.

$$\left[Vc_1^1, Vc_2^1, .., Vc_{NP}^1 \right] \tag{17}$$

The elements of the velocity vectors in each dimension are represented as:

$$Vc_j^1 = \left[vc_{j,1}^1, vc_{j,2}^1, .., vc_{j,Dv}^1 \right] \tag{18}$$

Odor particles help to predict the shark's progress toward its meal. When the odor concentration rises, the shark's speed increases since it is represented using a gradient-based objective function that determines the direction in which the highest rate occurs.

$$Vc_j^k = \xi_k . r . \nabla(OBJ)\Big|_{NP_j^k} \quad (19)$$

The SSO's function is shown by OBJ , ξ_k a value within the range of [0,1] [18] and r represents the random value between [0,1] the shark's speed is represented as Vc_j^k , where $k = 1,2,..., k_{\max}$ and $k_{\max}$ depicts the shark's forward motion, which may be separated into stages, with the stages being denoted by k and $\nabla(OBJ)$ depicting SSO's gradient.

When moving forward, the shark's location is denoted by Pw_j^{k+1}, which is calculated from the previous position and velocity, and is written as:

$$Pw_j^{k+1} = w_j^k + Vc_j^k . \Delta t_k \quad (20)$$

For the sake of simplicity, the time interval of stage k is treated in Equation 20 as Δt_k , with $\Delta t_k = 1$ at all stages. At each level, the shark conducts a local search to find the best possible solution, as indicated by Equation 21.

$$Ys_j^{k+1,u} = Pw_j^{k+1} + rn \cdot Pw_j^{k+1} \quad (21)$$

Here, term U denotes the quantity of points when the random variable $u = 1,2,..., U$ with an equal distribution identified as rn in the area Pw_j^{k+1} $[-1,+1]$, which is the native search U as a near point. These points are combined to create a closed loop that corresponds to the shark's rotational motion. When the shark detects a greater odor, it turns toward the spot in accordance with the rotational movement described by Equation 22.

$$w_j^{k+1} = \arg\max\left\{of\left(Pw_j^{k+1}\right), ob\left(Y_j^{k+1,1}\right), ..., ob\left(Y_j^{k+1,U}\right)\right\} \quad (22)$$

The positions of the shark are determined from the aforesaid equation as Pw_j^{k+1} positions attained by forward motion, known as $Ys_j^{k+1,U}$, and until k attains $k_{\max}$, the succession of forward and rotating motions continues. Ultimately, the ideal person is chosen as the SSO solution.

Additionally, the SSO update is done when $E_3 \geq 0.5$ in the S-BSO algorithm. To obtain food and improve survivability, the BSA uses bird behavior and social interactions, such as gathering behavior, vigilance behavior, and flight behavior. Assuming the virtual location of the swarm's number of birds is NP, $w_j^i = \left(w_{j,1}^i, w_{j,2}^i, \cdots, w_{j,K}^i\right)$ at time i for the j^{th} bird, $j \in [1,2,\cdots, NP]$, and $i \in [1,2,\cdots, j]$.

Hunting behavior: In individual and group experiences, each bird's foraging technique will determine how they go about finding food.

$$\begin{aligned} w_{j,m}^{i+1} &= w_{j,m}^i + \left(a_{j,m} - w_{j,m}^i\right) \times E \times rn(0,1) \\ &+ \left(b_m - w_{j,m}^i\right) \times C \times rn(0,1) \end{aligned} \quad (23)$$

Here, the letters E and C are numbers that represent the "social coefficients" and the "cognitive coefficients", respectively. The finest historical location for a bird is defined as $C = 1, a_{j,m}$, which is shared by the entire swarm at coordinate j^{th} fowl at the m^{th} coordinate, the uniformly distributed numbers are referred to as $rn(0,1)$, being in the bounding range of 0 and 1.

Behavior of alertness: The birds can approach the center of the swarm, and as a result, the motions of the birds are expressed in Equation 24.

$$w_{j,m}^{i+1} = w_{j,m}^{i} + F_1\left(mean_m - w_{j,m}^{i}\right)\times rn(0,1) + F_2\left(a_{x,m} - w_{j,m}^{i}\right)\times rn(-1,1) \quad (24)$$

$$F_1 = f1 \times \exp\left(-\frac{afit_j}{Sfit+\varepsilon}\times NP\right) \quad (25)$$

$$F_2 = a2 \times \exp\left[\left(\frac{afit_j - afit_x}{\left|afit_j - afit_x\right| + \varepsilon}\right)\frac{afit_j}{Sfit+\varepsilon}\times NP\right] \quad (26)$$

The mean location of the entire group at m^{th} coordinate is known as $mean_m$ and an integer is defined as x in the array of $[1, NP]$. The fitness cost for the finest historical location of the bird represents the totality of $afit_j$, $f1$ and $f2$ are the factors in the range used by Muhammad, et al. [19], and $x \neq j$ with ε added to the above equation to prevent a zero division error.

Flight pattern: The positions of producers and scroungers, two different bird species that make up a swarm population, are updated in Equations 27 and 28, respectively.

$$w_{j,m}^{i+1} = w_{j,m}^{i} \times rnh(0,1) \times w_{j,m}^{i} \quad (27)$$

$$w_{j,m}^{i+1} = w_{j,m}^{i} + \left(w_{x,m}^{i} - w_{j,m}^{i}\right)\times LE \times w_{j,m}^{i} \quad (28)$$

The scrounger learning efficiency (LE) is indicated by the LE by following the producer that is within the bounds of [0,2] Muhammad, et al. [19]. In Meng, et al. [27], a positive number is taken and assumes that every bird flies at dissimilar positions at the QP interval. The scavengers are instructed to follow any producer they come across; the producers, who resemble birds, represent the hungry people who are actively seeking food. By using random numbers, a fresh version of the S-BSO algorithm is run.

The proposed algorithm works by combining the best elements and values of the SSO and BSA approaches. The hybridization idea has been shown to provide superior convergence behavior in recent years [29]. In order to tackle the early convergence in adaptive beamforming of the millimetre-wave system for updated weights, a better convergence rate is achieved by the devised approach. Figure 2 presents the S-BSO algorithm's flowchart.

Minimizing the bit error rate (BER) in the millimeter-wave communication system is the main goal of the suggested S-BSO algorithm. In the millimeter wave model, the BER analysis aims to increase connection performance that, in turn, improves link connectivity. Therefore, reducing the bit error rate value guarantees the effectiveness of the suggested adaptive beamforming millimeter-wave communication model. Therefore, reducing the BER value ensures the efficacy of the proposed adaptive beamforming MMW communication model. Below is the main aim of the suggested S-BSO adaptive beamforming approach.

$$OBJ = \underset{\{w_k\}}{\arg\min}\,(BER) \quad (29)$$

$$BER = \frac{\rho_c}{\log_2 Sn} \quad (30)$$

The probability of symbol error in this context is denoted by ρ_c, which is the number of signals needed to represent the bits, shown as Sn, while the number of bits each signal can represent is given as $\log_2 Sn$. The suggested S-BSO adaptive beamforming approach aims to lower inaccuracies in MMW communication systems.

6. RESULTS AND DISCUSSIONS

The newly designed adaptive beamforming in millimeter-wave communication systems was implemented using MATLAB [30], and experimentation was done by changing the amount of RF chains and antennas. Performance of the recommended model was compared with the conventional models on the basis of convergence analysis. The population sizes of 10 and 100, as well as the maximum number of iterations, were considered. The developed model was compared with diverse optimization approaches such as the particle swarm optimization algorithm [31], the grey wolf optimization algorithm [32], SSO [28], and BSA [27], and classifiers such as YUWEI [33], General Eigen-Decomposition (GEVD) [34], CMA [35], and (LS-CMA) [36]. Three test cases were used to run this model, with antennas and RF chains set at 32, 48, and 64.

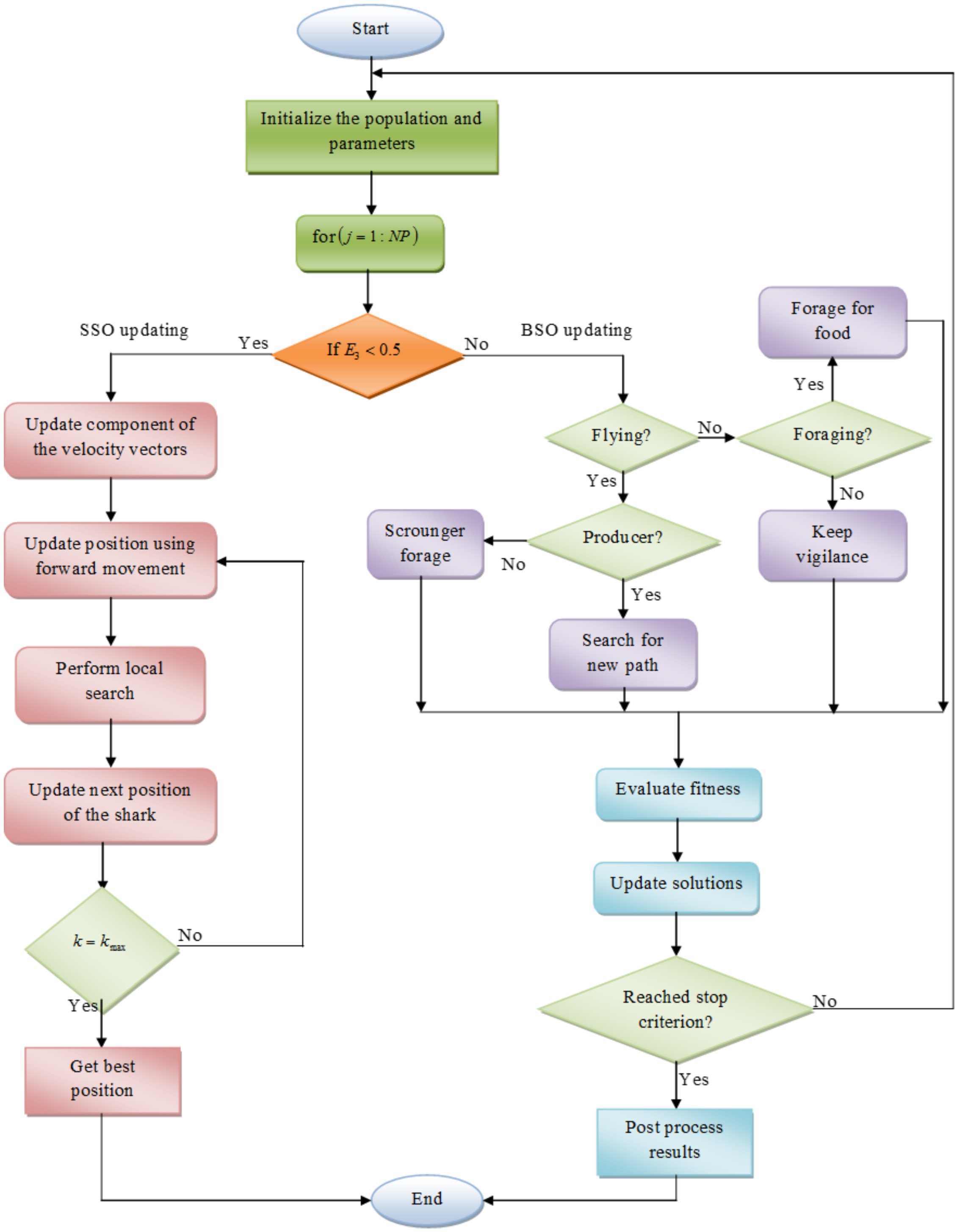

Figure 2. S-BSO algorithm flowchart.

A. Convergence Analysis

In Figure 3, calculated by adjusting the number of iterations, the convergence analysis of several adaptive beamforming algorithms is shown. The PSO, GWO, BSA, and SSO algorithms all use the S-BSO approach, which reaches a high convergence rate at the 25th iteration. The S-BSO algorithm's cost function is 75% better than PSO's, 79.5% better than GWO's, 80% better than SSO's, and 66.6% better than BSA's at the 100th iteration. As a result, the S-BSO algorithm's planned convergence rate is higher than that of other adaptive beamforming algorithms based on other optimization techniques.

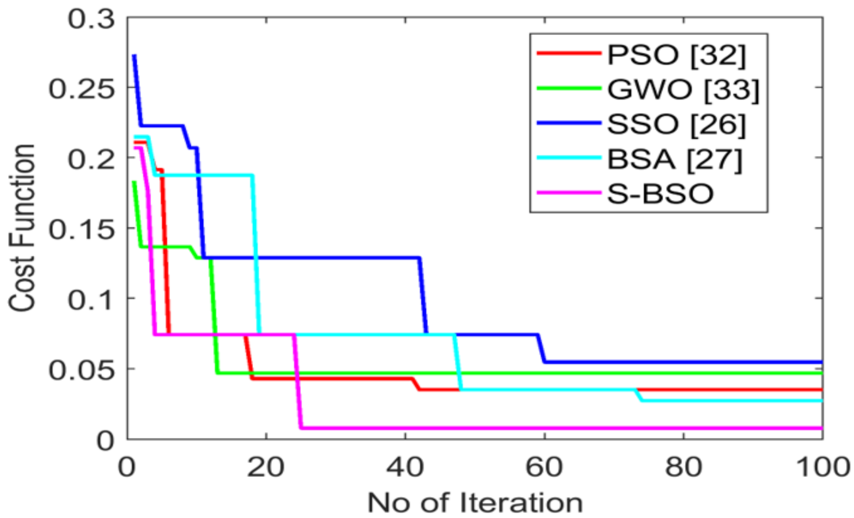

Figure 3. Using various optimization techniques, the convergence of several adaptive beamforming strategies in the MMW communication model is examined.

B. Analysis of Spectral Efficiency with Regard to SNR and Heuristic Methods

The suggested S-BSO method of adaptive beamforming performance, as given in Figure 4, is in relation to spectral efficiency. The suggested S-BSO methodology outperforms previous approaches in terms of spectrum efficiency. When the signal-to-noise ratio value is expected to be -15 and the set of antennas and RF chains is 32, it is 14.2% better than GWO and BSA, respectively. Similar to this, the adaptive beamforming utilizing the S-BSO approach has a spectral efficiency that is 11% and 48% higher than that of GWO and BSO, respectively, when 48 antennas and RF chains are used and the SNR value is -15. With 64 antennas and RF chains, and an SNR value of -15, adaptive beamforming employing the S-BSO approach outperforms BSA and GWO in terms of spectral efficiency by 14% and 17.6%, respectively. As a result, the suggested S-BSO algorithm for adaptive beamforming has more spectral efficiency than prior methods.

C. Analysis of BER to SNR

Figure 5 presents the bit error rate (the percentage of bits that have errors relative to the total number of bits received in a transmission) analysis with various traditional adaptive beamforming approaches. The BER is minimized in the novel S-BSO algorithm while comparing with an SNR value of -15 and RF chains and antenna are set at 32, which is 66.6%, 50%, 89.7%, and 76% better than the LS-CMA, GEVD, CMA and YUWEI algorithms. When the RF chain and antenna are set at 48, the bit error rate of the S-BSO algorithm is 14%, 60%, 20% and 9% better than the LS-CMA, GEVD, CMA and YUWEI, respectively. When the RF chain and antenna are set at 64, the bit error rate of the S-BSO algorithm is 20%, 53.8%, 75%, and 75% better than those of the YUWEI, GEVD, CMA and LS-CMA. So, the bit error rate of the S-BSO algorithm surpasses other conventional adaptive beamforming techniques.

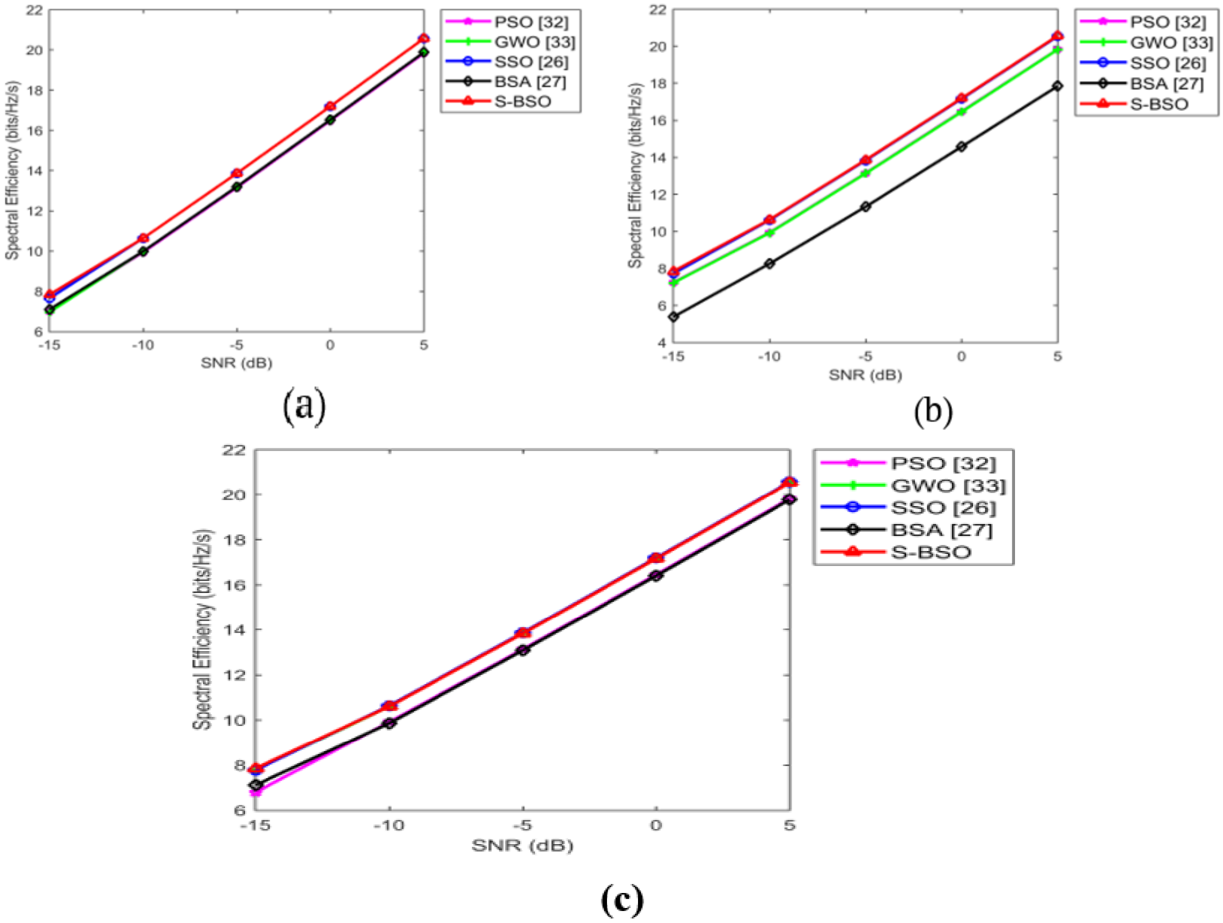

Figure 4. The spectral efficiency over SNR: (a) sets of RF chains and antennas are 32, (b) the sets of RF chains and antennas are 48, (c) the sets of RF chains and antennas are 64.

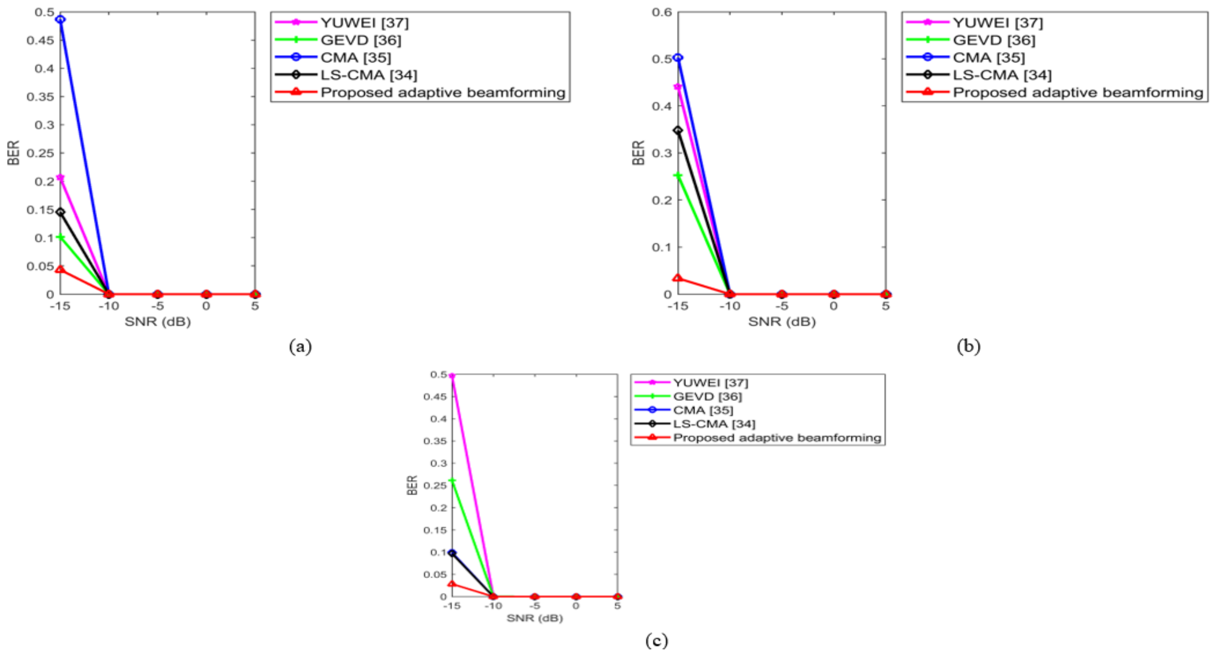

Figure 5. SNR over BER analysis: (a) the sets of RF chains and antennas are 32, (b) the sets of RF chains and antennas are 48, (c) the sets of RF chains and antennas are 64.

7. CONCLUSION

A novel S-BSO algorithm in the millimeter-wave communication system has been implemented using adaptive beamforming techniques. The S-BSO algorithm was primarily used in the suggested adaptive beamforming strategy to reduce the bit error rate in millimeter-wave communication model. The analysis of the bit error rate of the S-BSO adaptive beamforming algorithm improved the efficiency and performance of the MMW communication system. After comparing with conventional CMA, YUWEI GEVD and LS-CMA algorithms, the bit error rate of the S-BSO adaptive beamforming algorithm was 89.7%, 76%, 50%, and 66.6%. When 32 RF chains and antennas were used, the SNR (signal-to-noise ratio) value was taken into consideration. As a consequence, several evaluations have demonstrated that the suggested S-BSO-based adaptive beamforming approach outperforms the current beamforming techniques.

Funding: This study received no specific financial support.
Competing Interests: The authors declare that they have no competing interests.
Authors' Contributions: Both authors contributed equally to the conception and design of the study.

REFERENCES

[1] B. Yang, Z. Yu, J. Lan, R. Zhang, J. Zhou, and W. Hong, "Digital beamforming-based massive MIMO transceiver for 5G millimeter-wave communications," *IEEE Transactions on Microwave Theory and Techniques*, vol. 66, pp. 3403-3418, 2018.Available at: https://doi.org/10.1109/tmtt.2018.2829702.

[2] T. Bai and R. W. Heath, "Coverage and rate analysis for millimeter-wave cellular networks," *IEEE Transactions on Wireless Communications*, vol. 14, pp. 1100-1114, 2014.Available at: https://doi.org/10.1109/twc.2014.2364267.

[3] R. Zhang, J. Zhou, J. Lan, B. Yang, and Z. Yu, "A high-precision hybrid analog and digital beamforming transceiver system for 5G millimeter-wave communication," *IEEE Access*, vol. 7, pp. 83012-83023, 2019.Available at: https://doi.org/10.1109/access.2019.2923836.

[4] Z. Ma, B. Li, Z. Yan, and M. Yang, "QoS-Oriented joint optimization of resource allocation and concurrent scheduling in 5G millimeter-wave network," *Computer Networks*, vol. 166, p. 106979, 2020.Available at: https://doi.org/10.1016/j.comnet.2019.106979.

[5] H. Mohammadnezhad, R. Abedi, and P. Heydari, "A millimeter-wave partially overlapped beamforming-MIMO receiver: Theory, design, and implementation," *IEEE Transactions on Microwave Theory and Techniques*, vol. 67, pp. 1924-1936, 2019.Available at: https://doi.org/10.1109/tmtt.2019.2899322.

[6] W. Lu, W. Zou, and X. Liu, "An adaptive channel estimation algorithm for millimeter wave cellular systems," *Journal of Communications and Information Networks*, vol. 1, pp. 37-44, 2016.Available at: https://doi.org/10.1007/bf03391556.

[7] M. Haenggi, J. G. Andrews, F. Baccelli, O. Dousse, and M. Franceschetti, "Stochastic geometry and random graphs for the analysis and design of wireless networks," *IEEE Journal on Selected Areas in Communications*, vol. 27, pp. 1029-1046, 2009.Available at: https://doi.org/10.1017/cbo9781139043816.012.

[8] E. Turgut and M. C. Gursoy, "Coverage in heterogeneous downlink millimeter wave cellular networks," *IEEE Transactions on Communications*, vol. 65, pp. 4463-4477, 2017.Available at: https://doi.org/10.1109/glocom.2016.7841706.

[9] M. Giordani, M. Rebato, A. Zanella, and M. Zorzi, "Coverage and connectivity analysis of millimeter wave vehicular networks," *Ad Hoc Networks*, vol. 80, pp. 158-171, 2018.Available at: https://doi.org/10.1016/j.adhoc.2018.08.007.

[10] S. Rangan, T. S. Rappaport, and E. Erkip, "Millimeter-wave cellular wireless networks: Potentials and challenges," *Proceedings of the IEEE*, vol. 102, pp. 366-385, 2014.Available at: https://doi.org/10.1109/jproc.2014.2299397.

[11] M. R. Akdeniz, Y. Liu, M. K. Samimi, S. Sun, S. Rangan, T. S. Rappaport, and E. Erkip, "Millimeter wave channel modeling and cellular capacity evaluation," *IEEE Journal on Selected Areas in Communications*, vol. 32, pp. 1164-1179, 2014.Available at: https://doi.org/10.1017/9781009122740.006.

[12] H. ElSawy, E. Hossain, and M. Haenggi, "Stochastic geometry for modeling, analysis, and design of multi-tier and cognitive cellular wireless networks: A survey," *IEEE Communications Surveys & Tutorials*, vol. 15, pp. 996-1019, 2013.Available at: https://doi.org/10.1109/surv.2013.052213.00000.

[13] A. Alkhateeb, O. El Ayach, G. Leus, and R. W. Heath, "Channel estimation and hybrid precoding for millimeter wave cellular systems," *IEEE Journal of Selected Topics in Signal Processing*, vol. 8, pp. 831-846, 2014.

[14] J. G. Andrews, F. Baccelli, and R. K. Ganti, "A tractable approach to coverage and rate in cellular networks," *IEEE Transactions on Communications*, vol. 59, pp. 3122-3134, 2011.Available at: https://doi.org/10.1109/tcomm.2011.100411.100541.

[15] Z. Xiao, T. He, P. Xia, and X.-G. Xia, "Hierarchical codebook design for beamforming training in millimeter-wave communication," *IEEE Transactions on Wireless Communications*, vol. 15, pp. 3380-3392, 2016.Available at: https://doi.org/10.1109/twc.2016.2520930.

[16] L. Zhu, J. Zhang, Z. Xiao, X. Cao, D. O. Wu, and X.-G. Xia, "3-D beamforming for flexible coverage in millimeter-wave UAV communications," *IEEE Wireless Communications Letters*, vol. 8, pp. 837-840, 2019.Available at: https://doi.org/10.1109/lwc.2019.2895597.

[17] J. Treichler and B. Agee, "A new approach to multipath correction of constant modulus signals," *IEEE Transactions on Acoustics, Speech, and Signal Processing*, vol. 31, pp. 459-472, 1983.Available at: https://doi.org/10.1109/tassp.1983.1164062.

[18] J. Liu and E. S. Bentley, "Hybrid-beamforming-based millimeter-wave cellular network optimization," *IEEE Journal on Selected Areas in Communications*, vol. 37, pp. 2799-2813, 2019.Available at: https://doi.org/10.1109/jsac.2019.2947923.

[19] N. A. Muhammad, N. I. A. Apandi, Y. Li, and N. Seman, "Uplink performance analysis for millimeter wave cellular networks with clustered users," *IEEE Transactions on Vehicular Technology*, vol. 69, pp. 6178-6188, 2020.Available at: https://doi.org/10.1109/tvt.2020.2980291.

[20] M. Cheng, J.-B. Wang, Y. Wu, X.-G. Xia, K.-K. Wong, and M. Lin, "Coverage analysis for millimeter wave cellular networks with imperfect beam alignment," *IEEE Transactions on Vehicular Technology*, vol. 67, pp. 8302-8314, 2018.Available at: https://doi.org/10.1109/tvt.2018.2842213.

[21] F. E. Asim, F. Antreich, C. C. Cavalcante, A. L. de Almeida, and J. A. Nossek, "Channel parameter estimation for millimeter-wave cellular systems with hybrid beamforming," *Signal Processing*, vol. 176, p. 107715, 2020.Available at: https://doi.org/10.1016/j.sigpro.2020.107715.

[22] Q. Sultan, M. S. Khan, and Y. S. Cho, "Fast 3D beamforming technique for millimeter-wave cellular systems with uniform planar arrays," *IEEE Access*, vol. 8, pp. 123469-123482, 2020.Available at: https://doi.org/10.1109/access.2020.3006216.

[23] K. Satyanarayana, M. El-Hajjar, P. Kuo, A. Mourad, and L. Hanzo, "Hybrid beamforming design for full-duplex millimeter wave communication," *IEEE Transactions on Vehicular Technology*, vol. 68, pp. 1394-1404, 2019.

[24] W. Wang, W. Zhang, and J. Wu, "Optimal beam pattern design for hybrid beamforming in millimeter wave communications," *IEEE Transactions on Vehicular Technology*, vol. 69, pp. 7987-7991, 2020.Available at: https://doi.org/10.1109/tvt.2020.2992534.

[25] M. N. Kulkarni, A. Ghosh, and J. G. Andrews, "A comparison of MIMO techniques in downlink millimeter wave cellular networks with hybrid beamforming," *IEEE Transactions on Communications*, vol. 64, pp. 1952-1967, 2016.Available at: https://doi.org/10.1109/tcomm.2016.2542825.

[26] B. Agee, "The least-squares CMA: A new technique for rapid correction of constant modulus signals," in *Proc. IEEE Int. Conf. Acoust. Speech Signal Process*, 1986, pp. 953–956.

[27] X.-B. Meng, X. Z. Gao, L. Lu, Y. Liu, and H. Zhang, "A new bio-inspired optimisation algorithm: Bird Swarm Algorithm," *Journal of Experimental & Theoretical Artificial Intelligence*, vol. 28, pp. 673-687, 2016.Available at: https://doi.org/10.1080/0952813x.2015.1042530.

[28] O. Abedinia, N. Amjady, and A. Ghasemi, "A new metaheuristic algorithm based on shark smell optimization," *Complexity*, vol. 21, pp. 97-116, 2016.Available at: https://doi.org/10.1002/cplx.21634.

[29] M. M. Beno, V. I. R, S. S. M, and B. Rajakumar, "Threshold prediction for segmenting tumour from brain MRI scans," *International Journal of Imaging Systems and Technology*, vol. 24, pp. 129-137, 2014.Available at: https://doi.org/10.1002/ima.22087.

[30] MATLAB, "Natick, Massachusetts: The MathWorks Inc. Retrieved: https://www.mathworks.com/products/new_products/release2020a.html," 2020a.

[31] N. Jin and Y. Rahmat-Samii, "Advances in particle swarm optimization for antenna designs: Real-number, binary, single-objective and multiobjective implementations," *IEEE Fransactions on Antennas and Propagation*, vol. 55, pp. 556-567, 2007.Available at: https://doi.org/10.1109/tap.2007.891552.

[32] S. Mohanty, B. Subudhi, and P. K. Ray, "A new MPPT design using grey wolf optimization technique for photovoltaic system under partial shading conditions," *IEEE Transactions on Sustainable Energy*, vol. 7, pp. 181-188, 2015.Available at: https://doi.org/10.1109/tste.2015.2482120.

[33] Y. Ren, Y. Wang, C. Qi, and Y. Liu, "Multiple-beam selection with limited feedback for hybrid beamforming in massive MIMO systems," *IEEE Access*, vol. 5, pp. 13327-13335, 2017.Available at: https://doi.org/10.1109/access.2017.2666782.

[34] T. Lin, J. Cong, Y. Zhu, J. Zhang, and K. B. Letaief, "Hybrid beamforming for millimeter wave systems using the MMSE criterion," *IEEE Transactions on Communications*, vol. 67, pp. 3693-3708, 2019.Available at: https://doi.org/10.1109/tcomm.2019.2893632.

[35] F. Colone, R. Cardinali, P. Lombardo, O. Crognale, A. Cosmi, A. Lauri, and T. Bucciarelli, "Space–time constant modulus algorithm for multipath removal on the reference signal exploited by passive bistatic radar," *IET Radar, Sonar & Navigation*, vol. 3, pp. 253-264, 2009.Available at: https://doi.org/10.1049/iet-rsn:20080102.

[36] V. Dakulagi and M. Bakhar, "Efficient blind beamforming algorithms for phased array and MIMO RADAR," *IETE Journal of Research*, vol. 64, pp. 241-246, 2018.Available at: https://doi.org/10.1080/03772063.2017.1351319.